RESEARCH PAPER

Selective adsorption of solvents in a multiscale device

Torsten Henning · Juergen J. Brandner · Lutz Eichhorn · Klaus Schubert ·
Martin Schreiber · Martin Güngerich · Hermann Günther · Peter J. Klar ·
Vivian Rebbin · Michael Fröba

Abstract We have incorporated microspheres, from 50 to 80 μm in diameter, of periodic mesoporous organosilica (inner surfaces up to 1,000 m^2/g and pore sizes in the nanometre range) with two types of organic functionalities (benzene and ethane bridges, respectively) inside microstructured channels (each 200 μm wide and 100 μm deep) and, exemplarily, monitored by Raman microscopy (Raman spectroscopy through microscope optics) that the temperature characteristics of the adsorption–desorption equilibria of benzene and ethanol vary significantly with the type of organic functionality of the microspheres and the pore morphology. The integration of this class of nanostructured material into devices by means of microchannels is a promising novel approach to, among others, substance separation in analytics, micro process engineering, and micro chemistry.

List of symbols
p pressure (Pa)
P power (W)
T temperature (°C)
λ wave length (m)

T. Henning (✉) · J. J. Brandner · L. Eichhorn ·
K. Schubert
Forschungszentrum Karlsruhe GmbH,
Institute for Micro Process Engineering IMVT,
76344 Eggenstein-Leopoldshafen, Germany
e-mail: Torsten.Henning@exp1.physik.uni-giessen.de

M. Schreiber · M. Güngerich · H. Günther · P. J. Klar
Department of Physics and Material Sciences,
Philipps-University, 35032 Marburg, Germany
e-mail: Peter.J.Klar@exp1.physik.uni-giessen.de

V. Rebbin · M. Fröba
Institute of Inorganic and Analytical Chemistry,
Justus-Liebig-University, 35392 Giessen, Germany
e-mail: michael.froeba@anorg.chemie.uni-giessen.de

Present Address:
T. Henning · P. J. Klar
Physics Institute I, Justus-Liebig-University,
35392 Giessen, Germany

1 Introduction

For a variety of applications in chemical analysis as well as synthesis, miniaturised systems (Hessel et al. 2005; Schubert et al. 2001) are preferable for a number of reasons, such as enhanced flexibility, speed or yield, reduced consumption of reactants, safety, etc. In this context, it is desirable to miniaturise as many of the components as possible in a modular fashion so that integration to systems is facilitated. While considerable progress has been made in the miniaturisation of micromechanical and microfluidic devices, other components, in particular those relying on chemical or physical interactions between supplied reactants and the system surface, require further development.

Open framework materials with functionalisation via guest molecules have shown the possibility of being engineered for specific applications (Janiak 2003),

exemplified by selective solvent sorption (Choi et al. 2004). Novel porous materials with characteristic pore sizes between 2 and 20 nm based on mesoporous silica synthesized with supramolecular structure-directing agents via a self assembled liquid–crystalline templating route (Kresge et al. 1992) offer promising perspectives for microdevices. These materials show large inner surface areas (>500 m^2/g), highly ordered pore systems and the possibility of a targeted functionalisation with chemically active groups. A novel subgroup is the so-called periodic mesoporous organosilica (PMO) (Hoffmann et al. 2006a) in which the organic functionality of the pore system is achieved by spatially regular incorporation of organic molecules as part of the pore walls themselves. By varying the synthesis conditions, the macroscopic shape of the PMO material can be controlled, i.e., microspheres, thin films on substrates as well as monolithic structures can be created. In addition to a control of the pore sizes, the diameter of PMO microspheres is accurately adjustable in the size range of 500 nm to 500 μm, and the distribution of sizes for any given parameter set is narrow around the respective mean diameter (Rebbin et al. 2004).

2 Experimental setup and procedure

Figures 1, 2 and 3 are an illustration the multi-scale integration scheme we employed for a controlled incorporation of functionalised nanostructures into a device with microchannels. PMO microspheres with nanosized pores are immobilised inside these microchannels by a narrow channel retainer structure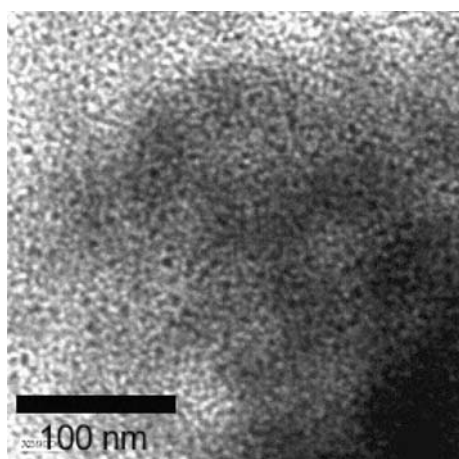 located downstream. Figure 1 is a transmission electron micrograph of a microsphere, clearly showing the system of nanosized pores (for the determination of pore sizes and their distribution, see below). Figure 2 shows a detail view of a microchannel outlet with the narrow channel retainer, imaged by scanning electron microscopy. The microspheres integrated into one of the microchannels are shown in the optical microscopy image in Fig. 3.

2.1 Synthesis and characterisation of PMO microspheres

The PMO microspheres were synthesised by solving different ratios of dodecylamine in a mixture of ethanol and 1,4-bis(triethoxysilyl)benzene (BTEB) for benzene-bridged PMOs and 1,2-bis(triethoxysilyl)ethane (BTEE) for ethane-bridged PMOs. A mixture of hydrochloric acid and water was added to the clear solution of the precursor, the solvent and the structure directing agent. A white precipitation occurred almost immediately. Samples with BTEB were stirred for additional 75 min with 500 rpm. Samples containing BTEE were stirred for 2 h with 300 rpm. After the stirring time the formation of the microspheres is complete. A hydrothermal treatment is not necessary. The white solid is then washed with water and ethanol and dried overnight in air. Removal of the structure directing agent is accomplished by solvent extraction with ethanol/HCl (100:3; v:v) in a Soxhlet apparatus for 6 h. Then the solid is washed again and dried in air to yield the microspheres in the size range from 50 to 80 μm.
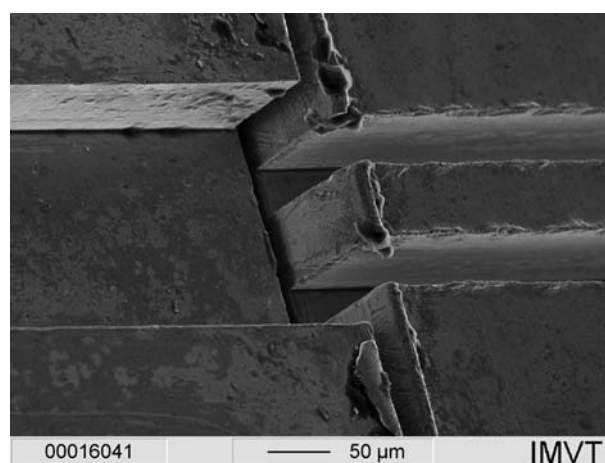

Fig. 1 Transmission electron micrograph of a single PMO microsphere

Fig. 2 Scanning electron micrograph of a mechanically micromachined, wider channel end (*left*) prior to the filling with the microspheres, and the narrow channel retainer structure (*right*), also mechanically micromachined, designed to keep the microspheres inside the wider channel
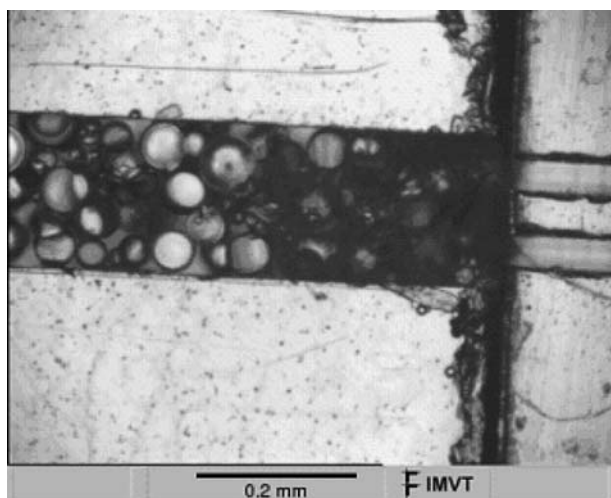
Fig. 3 Optical micrograph of one of the wider channels, filled with PMO microspheres (*left*), and the retainer structure (*right*)

Both PMO materials do not show any indication of a regular mesopore arrangement in the powder X-ray diffraction (P-XRD) patterns (not shown) as probably expected due to the spherical shape. Nitrogen physisorption measurements were carried out in order to obtain information about the pore diameter, the pore-size distribution, and the specific surface areas of the benzene-bridged and the ethane-bridged sample. The measured isotherms and the corresponding pore-size distributions calculated by the NLDFT method are shown in the top and the bottom graph of Fig. 4, respectively. The isotherm obtained for the ethane-bridged sample is a type IV isotherm, which is typical for mesoporous materials. The shape of the isotherm is in concordance with the results of the corresponding P-XRD measurement. The pores of the ethane-bridged PMO are fairly disordered and the resulting pore size distribution is rather broad similar to samples synthesised via sol-gel reaction procedures. The specific surface area (calculated by the BET method) is about 1,000 m^2/g. The isotherm of the benzene-bridged samples is a typical type I isotherm. The resulting pore size distribution is much sharper with a distinct maximum at a diameter of about 1.5 nm, which is still in the micropore range. The pore-size distribution is narrow, no pores larger than 4 nm are observed. The calculated specific surface area is about 600 m^2/g. The observed differences in the pore diameter and the shape of the isotherm can be explained in terms of the different flexibility of the organosilica precursors and the different reaction speeds in the synthesis of the two organic bridges.

^{29}Si-MAS-NMR investigations confirm the stability of the organic bridges in both materials, i.e., the Si–C

bond is not cleaved during the reaction or the extraction procedure. The thermal stability was proved by thermogravimetric analysis. The ethane bridged sample starts to decompose at a temperature of about 250°C. The thermal stability of the benzene-bridged sample is considerably higher (up to 450°C) because of the high thermal stability of the aromatic system.

2.2 Micromachining and reactor assembly

An array of seven microchannels, each 200 μm wide and 100 μm deep was machined by micromilling with a rotating tool into a brass plate of 5 mm thickness. At the downstream end of these 200 μm channels, the brass plate contained a recess into which the separately micromachined retainer structure was inserted. This retainer structure was manufactured by microcutting in brass and comprised two high aspect ratio microchannels of only 40 μm width and 100 μm depth, separated by a ridge of 60 μm width, for each of the seven 200 μm wide microchannels (Fig. 2). To enable optical access for in situ measurements, the microchannel array was covered by a glass plate sealed by a polymeric gasket. The microstructured plate was fixed on a stainless steel base providing fluidic connections with standard fittings. The temperature of the reactor channel array was monitored by two thermocouples located just below the brass plate, and was electronically controlled via an electrical heater cartridge with integrated thermocouple inserted in the steel base block.

The 200 μm wide channels were loaded with PMO by injecting a suspension of a mixture of ethane-bridged and benzene-bridged PMO microspheres in ethanol into the assembled reactor via the fluidic inlet. The ethanol was then driven out by heating and flushing with nitrogen gas for several hours. The 40 μm narrow channel retainer structures reliably immobilised the PMO microspheres inside the 200 μm wide channels (Fig. 3).

2.3 Measurement of the net-adsorption of solvents

Figure 5 depicts schematically the set-up used for the temperature-dependent measurements of the net-adsorption of a solvent (benzene or ethanol) by the mixture of ethane-bridged and benzene-bridged PMO microspheres at adsorption-desorption equilibrium. Nitrogen gas was led through a flask with the solvent at 20°C. The outlet of the flask was connected to the inlet of the reactor which was kept at a constant temperature in the range between 20 and 140°C. The nitrogen gas enriched with solvent vapour was led over the two types of microspheres inside the reactor channel and
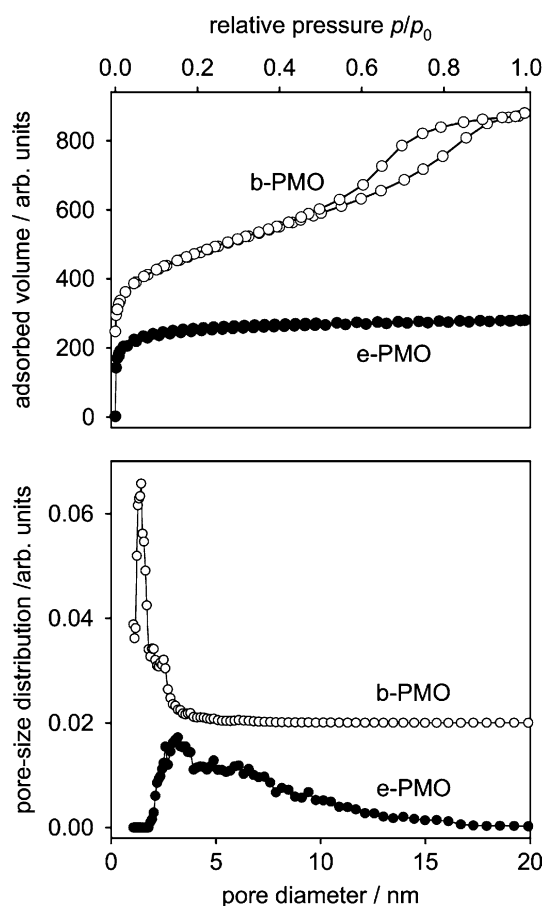
Fig. 4 *Top* Nitrogen physisorption isotherms of benzene- and ethane-bridged PMO. *Bottom* corresponding pore-size distribution calculated by the NLDFT method
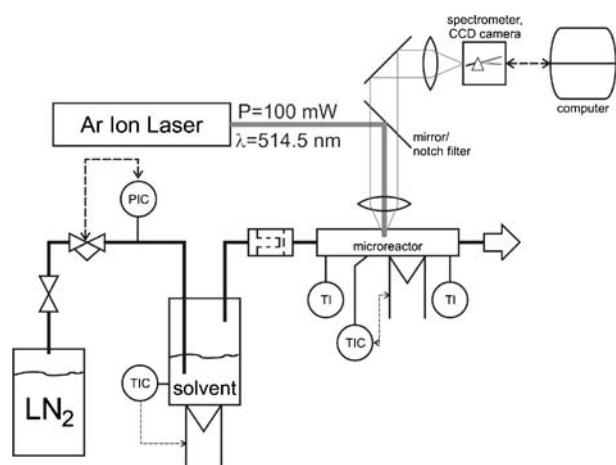

Fig. 5 Experimental setup for the in-situ Raman measurements. The solvent flask temperature control was not used in the set of measurements described in this paper

dumped into an exhaust at ambient pressure. The pressure inside the reactor in the region of the microspheres was a few tens of Pa above ambient pressure.

To monitor the net-adsorption of the vapour by individual PMO microspheres at different temperatures, micro-Raman measurements were performed in backscattering geometry using a Jobin Yvon microscope system. Excitation light (514.5 nm) of an air-cooled Ar^+ laser was coupled via optical fibres into the microscope system and focussed onto an individual PMO sphere inside the 200 μm channels. The laser power on the sample was kept below 20 mW to avoid laser-induced annealing. The scattered light was collected via the same microscope objective.

Elastically scattered laser light was rejected by a Kaiser optics holographic notch filter before coupling the Raman-scattered light into the spectrometer system (Acton Research Corporation SpectraPro-500). The spectra were detected by a liquid nitrogen cooled ISA CCD2000 CCD camera. Typical recording times for a spectrum were 6 min. At each temperature, it was assured that the adsorption of the solvent vapour by the PMO microsphere under study was in the steady state.

3 Results and discussion

Exemplarily, Fig. 6 depicts the Stokes Raman spectra of liquid benzene, of liquid ethanol and of PMO spheres functionalised by benzene bridges and ethane bridges, respectively. All four Raman spectra exhibit characteristic features (e.g., the peaks labelled a and f), which allow one to distinguish between the four substances (Dollish et al. 1974; Hoffmann et al. 2006b). In particular, it enables one to identify individual PMO spheres in the mixture inside the reactor channel as well as to detect solvent vapour adsorbed by a PMO sphere. In the following we will show that a careful analysis of the latter can be employed for extracting the temperature characteristics of the solvent adsorption by a PMO material from a series of Raman spectra taken on an individual PMO sphere inside the microreactor at different temperatures.

Information about the temperature dependent behaviour of the amount of solvent (here: benzene or ethanol) adsorbed by a PMO (here, either benzene-bridged or ethane-bridged) can be obtained because the Raman spectrum of the solvent adsorbed by the PMO microspheres is not significantly altered compared to that of liquid solvent as the adsorption and desorption processes are of physical origin (i.e., no chemical transformation of the adsorbant takes place). Furthermore, Stokes-Raman spectra, which involve the creation of vibrational quanta, are to a first approximation independent of temperature. Therefore, the
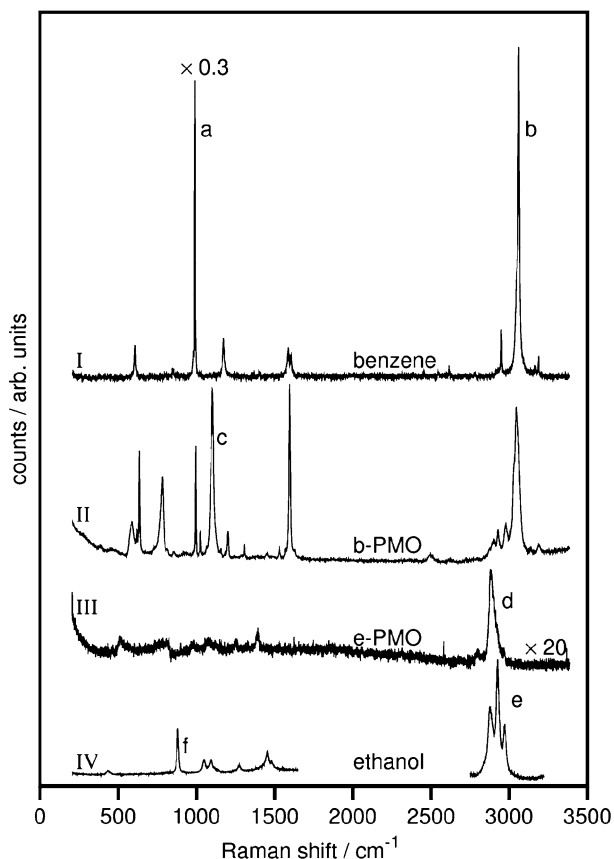
Fig. 6 Raman spectra of (*I*) liquid benzene, (*II*) a benzene-bridged-PMO microsphere, (*III*) an ethane-bridged PMO microsphere, and (*IV*) liquid ethanol. All spectra were taken at room temperature (20°C)

intensity ratio of a characteristic solvent peak and a characteristic PMO peak in the spectrum of a PMO microsphere inside the reactor is a measure for the amount of benzene adsorbed by the microsphere in the steady state.

We have chosen the following peak ratios in the four cases: (1) benzene adsorbed by benzene-bridged PMOs: ratio a:c ; (2) ethanol adsorbed by benzene-bridged PMOs: ratio f:c ; (3) benzene adsorbed by ethane-bridged PMOs: ratio b:d ; (4) ethanol adsorbed by ethane-bridged PMOs: ratio e:d . In the first three cases the evaluation is straight forward as the corresponding peaks in the spectra are spectrally separated (see also Fig. 6). Therefore, and because the line width of the Raman signals does not change with temperature, it is sufficient to analyze the ratio of the peak intensities for determining the characteristic adsorption curve of the solvent. In the fourth case, the analysis is more involved because the Raman signals (group of three peaks e and peak d in Fig. 6) spectrally overlap. For extracting the peak ratio we have fitted the spectra taken inside the microreactor at different

temperatures by a linear combination of spectra (III) and (IV) in Fig. 6 using a least-squares routine.

As examples, Figs. 7 and 8 depict two series of Raman spectra taken of PMO microspheres in a benzene environment inside the microreactor at different temperatures. The series in Fig. 7 was acquired on an individual benzene-bridged PMO microsphere whereas the series in Fig. 8 was taken on an individual ethane-bridged microsphere. Spectra taken with the laser spot focussed onto the gas flow alone yielded no benzene signals. Therefore, the benzene signals a and b in the spectra acquired when focussing on individual benzene-bridged and ethane-bridged PMO spheres, respectively, are indicative for the amount of benzene adsorbed by the microsphere.

It can be seen in Fig. 7 that the amount of benzene adsorbed by the b-PMO microsphere decreases, though weakly, with increasing reactor temperature. A considerable amount of benzene is still adsorbed at the highest reactor temperature of 113°C as is clearly
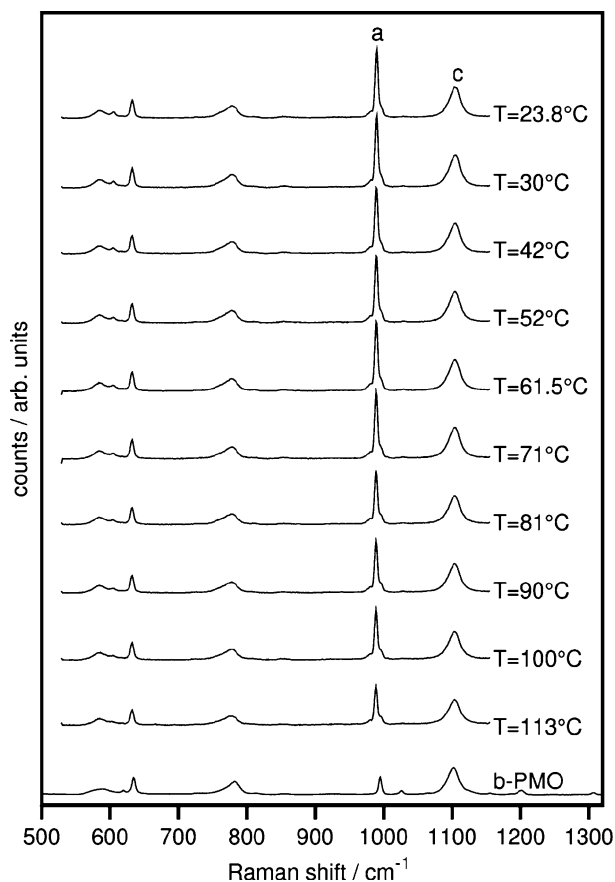

Fig. 7 Series of Raman spectra of a benzene-bridged PMO microsphere with adsorbed benzene vapour taken inside the microreactor at different temperatures in the range from 23.8 to 113°C. The bottom spectrum is that of the plain PMO microsphere. The characteristic features used in the evaluation of the adsorption behaviour are labelled *a* and *c*

visible when comparing the corresponding Raman spectrum with that of the pure benzene-bridged PMO (two spectra at the bottom of the figure). The adsorption behaviour of benzene by ethane-bridged PMO microspheres is quite different as illustrated by the relative intensity changes of peak b and d in Fig. 8. The intensity of the benzene peak b changes by almost a factor of 4 compared to the reference peak d of the ethane-bridged PMO (Fig. 8) whereas the benzene peak a only changed by about a factor of 2 in the same temperature range with respect to the reference peak c of the benzene-bridged PMO (Fig. 7). Again by comparing the two lowest spectra in Fig. 8 one finds that even at the reactor temperature of 122.5°C some benzene remains adsorbed by the ethane-bridged PMO.

A comparison of the absolute intensities of the benzene-vapour peaks a and b detected on a benzene-bridged PMO and an ethane-bridged PMO, respectively, allows one to even compare the absolute
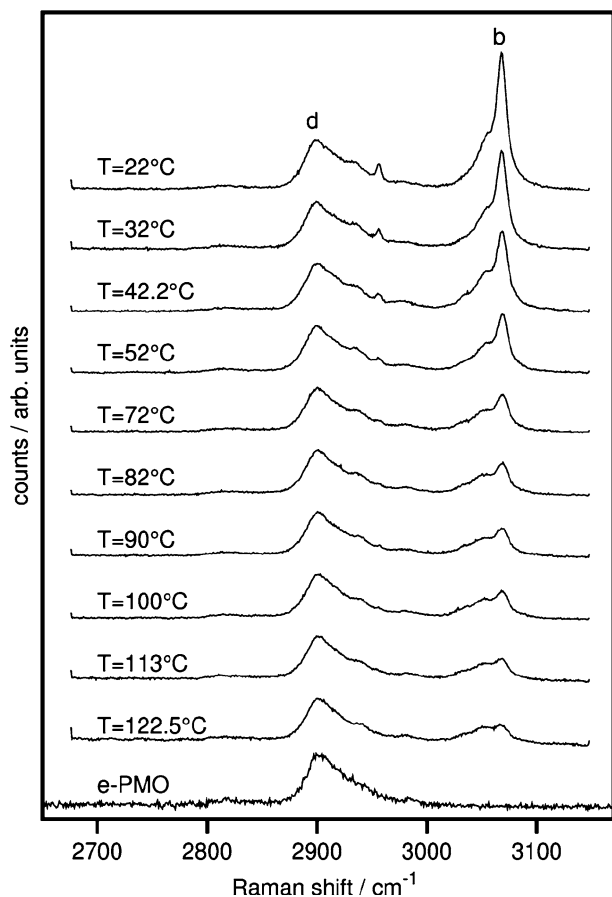
adsorption capabilities of the two types of PMO spheres. In a similar fashion, the absolute adsorption capability of ethanol by the two types of PMO spheres can be determined. All values are normalised to the active inner surface.

Figure 9 depicts the temperature-dependent net-adsorption of benzene (left) and of ethanol (right) by the two types of PMO microspheres, which were determined as described above. The net-adsorption behaviour of both solvents varies with the type of PMO. When adsorbed by the ethane-bridged PMOs a positive curvature of the temperature dependence is observed and the amount of adsorbed benzene (ethanol) drops by a factor of 3 (5) between 20 and 120°C (30 and 130°C). In contrast, a negative curvature of the temperature dependent net adsorption is observed for both solvents in case of the benzene-bridged PMOs.

The amount of adsorbed benzene only drops by a factor of 1.8 between 20 and 120°C and is almost constant up to 70°C. The amount of adsorbed ethanol changes by a factor of 4 between 20 and 100°C. It is worth noting that for both solvents the absolute amount adsorbed at 20°C by the ethane-bridged PMOs is twice as large as that absorbed by the benzene-bridged PMOs, even after correction for the active surface. For each solvent the adsorption characteristics of the two types of PMO can be directly compared as the curves were obtained at the same solvent partial pressure in the reactor. Therefore, the observed differences must be due to differences in pore morphology and chemical interactions.

For example, let us consider a benzene molecule, which has a diameter of about 0.46 nm, inside a 2 nm
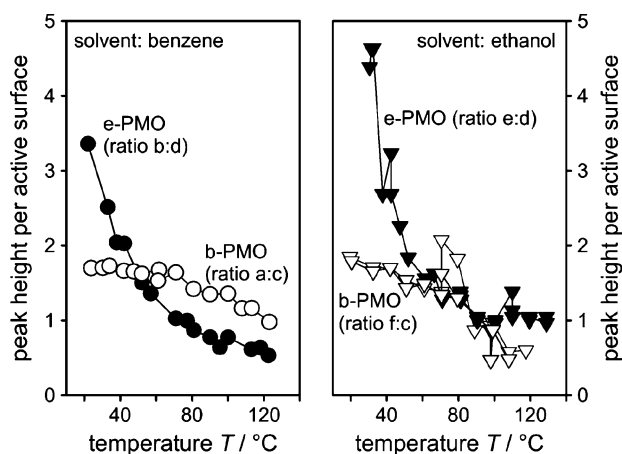

Fig. 8 Series of Raman spectra of an ethane-bridged PMO microsphere with adsorbed benzene vapour taken inside the microreactor at different temperatures in the ranging from 22 to 122.5°C. The bottom spectrum is that of the plain PMO microsphere. The characteristic features used in the evaluation of the adsorption behaviour are labelled b and d

Fig. 9 Temperature dependence of the solvent-vapour adsorption capabilities of PMO microspheres with ethane bridges (e-PMO) and benzene bridges (b-PMO), respectively. Letters a to f refer to the peak labels in (6). *Left* net adsorption of benzene, *right* net adsorption of ethanol

pore of benzene-bridged PMO. If the pore-wall surface is covered with benzene, at most 4 additional molecules have space in a typical cross section of the pore. Thus, the diffusion of the molecules in and out of the completely filled pore system will be inhibited. The pore system of the ethane-bridged PMO with 6 nm diameter cannot be blocked as easily. This explains why the amount of benzene adsorbed at 20°C by the benzene-bridged PMO is smaller than for the ethane-bridged PMO despite the strong p–p interaction of the benzene molecules with the pore walls of benzene-bridged PMO. The weaker temperature dependence of the net-absorption compared with the ethane-bridged PMO is also partly due to the pore size effect. In addition, there is a contribution due to differences in the chemical interaction between the benzene and the pore walls. It is dominated by the strong p–p interaction in the benzene-bridged PMOs whereas for the ethane-bridged PMOs the much weaker interaction between the aromatic benzene and the silanol groups is dominant.

The same arguments in terms of the pore morphology hold for adsorption of ethanol molecules by the two types of PMOs. This is the cause of the strong similarities between the left and right graph of Fig. 9. In contrast to benzene, the dominant chemical interaction between ethanol and both PMOs is hydrogen bonding with the silanol groups. This difference in chemical interactions as well as solvent partial pressure will explain to a large extent the remaining differences between the two graphs of Fig. 9, e.g., why the net-desorption rate of ethanol from the benzene-bridged PMOs is twice as large than the corresponding one of benzene.

4 Conclusions

We have developed a novel versatile approach of integrating periodic mesoporous organosilica (PMO) into a macroscopic device by using microstructured components. The incorporation of PMO microspheres inside the reactor channels not only yields new functionalities, but also leads to an effective enhancement of the active reactor surface by many orders of magnitude.

Our results demonstrate that the adsorption behaviour of reactants not only depends on the functionalisation of the PMO, but also on the pore morphology. The strong temperature dependence of the adsorption we observed offers the prospect of temperature modulated adsorption–desorption based devices, which will be able to work at short cycle times due to the low

thermal mass of the microreactor employed (Brandner et al. 2004).

To date, almost 50 differently functionalised PMOs have already been reported in the literature (Hoffmann et al. 2006a). This suggests that there is great potential for the implementation of a wide range of physico–chemical operations even beyond the selective separation of solvent vapours and nitrogen gas demonstrated here.

Systematic studies of the influence of pore topology and pore functionalisation on the temperature dependent equilibrium adsorption should provide the basis for a theoretical modelling of devices. More data is urgently needed to achieve a sufficient understanding of the processes underlying adsorption–desorption based devices with PMOs as active material.

References

Brandner JJ, Emig G, Liauw MA, Schubert K (2004) Fast temperature cycling in microstructure devices. Chem Eng J 101:217–224. DOI: 10.1016/j.cej.2003.11.020

Choi EY, Park K, Yang CM, Kim H, Son JH, Lee SW, Lee YH, Min D, Kwon YU (2004) Benzene-templated hydrothermal synthesis of metal-organic frameworks with selective sorption properties. Chem Eur J 10:5535–5540. DOI: 10.1002/chem.200400178

Dollish FR, Fateley WG, Bentley FF (1974) Characteristic Raman frequencies of organic compunds. Wiley, New York

Hessel V, Löwe H, Müller A, Kolb G (2005) Chemical micro process engineering, Wiley-VCH. DOI: 10.1002/3527603581

Hoffmann F, Cornelius M, Morell J, Fröba M (2006a) Periodic mesoporous organosilicas (PMOs): past, present, and future. J Nanosci Nanotech 6:265–288. DOI: 10.1166/jnn.2006.001

Hoffmann F, Güngerich M, Klar PJ, Fröba M (2006b) Vibrational spectroscopy of periodic mesoporous organosilica (PMOs) and their precursors—a closer look. Unpublished

Janiak C (2003) Engineering coordination polymers towards applications. Dalton Trans: 2781–2804. DOI: 10.1039/b305705b

Kresge CT, Leonowicz ME, Roth WJ, Vartuli JC, Beck JS (1992) Ordered mesoporous molecular sieves synthesized by a liquid–crystal template mechanism. Nature 359:710–711. DOI: 10.1038/359710a0

Rebbin V, Jakuboswki M, Pötz S, Fröba M (2004) Synthesis and characterisation of spherical periodic mesoporous organosilicas (sph-PMOs) with variable pore diameters. Microporous Mesoporous Mater 72:99–104. DOI: 10.1016/j.micromeso.2004.04.018

Schubert K, Brandner J, Fichtner M, Linder G, Schygulla U, Wenka A (2001) Microstructure devices for applications in thermal and chemical process engineering. Microscale Thermophys Eng 5:17–39. DOI: 10.1080/108939501300005358